

## Article

# Deposition of 3YSZ-TiC PVD Coatings with High-Power Impulse Magnetron Sputtering (HiPIMS)

Bastian Gaedike <sup>1,\*</sup>, Svenja Guth <sup>2</sup>, Frank Kern <sup>2</sup> , Andreas Killinger <sup>2</sup> and Rainer Gadow <sup>2</sup><sup>1</sup> Hartmetall-Werkzeugfabrik Paul Horn GmbH, 72072 Tuebingen, Germany<sup>2</sup> Institute for Manufacturing Technologies of Ceramic Components and Composites (IFKB), University of Stuttgart, Allmandring 7b, 70569 Stuttgart, Germany; svenja.guth@posteo.de (S.G.); frank.kern@ifkb.uni-stuttgart.de (F.K.); andreas.killinger@ifkb.uni-stuttgart.de (A.K.); rainer.gadow@ifkb.uni-stuttgart.de (R.G.)

\* Correspondence: bastian.gaedike@phorn.de

**Abstract:** Optimized coating adhesion and strength are the advantages of high-power impulse magnetron sputtering (HiPIMS) as an innovative physical vapor deposition (PVD) process. When depositing electrically non-conductive oxide ceramics as coatings with HiPIMS without dual magnetron sputtering (DMS) or mid-frequency (MF) sputtering, the growing coating leads to increasing electrical insulation of the anode. As a consequence, short circuits occur, and the process breaks down. This phenomenon is also known as the disappearing anode effect. In this study, a new approach involving adding electrically conductive carbide ceramics was tried to prevent the electrical insulation of the anode and thereby guarantee process stability. Yttria-stabilized zirconia (3YSZ) with 30 vol.% titanium carbide (TiC) targets are used in a non-reactive HiPIMS process. The main focus of this study is a parameter inquisition. Different HiPIMS parameters and their impact on the measured current at the substrate table are analyzed. This study shows the successful use of electrically conductive carbide ceramics in a non-conductive oxide as the target material. In addition, we discuss the observed high table currents with a low inert gas mix, where the process was not expected to be stable.

**Keywords:** coating characterization; disappearing anode effect; electrically conductive additives; HiPIMS parameters; yttria-stabilized zirconia



**Citation:** Gaedike, B.; Guth, S.; Kern, F.; Killinger, A.; Gadow, R. Deposition of 3YSZ-TiC PVD Coatings with High-Power Impulse Magnetron Sputtering (HiPIMS). *Appl. Sci.* **2021**, *11*, 2753. <https://doi.org/10.3390/app11062753>

Academic Editor: Yuzo Nakamura

Received: 30 December 2020

Accepted: 17 March 2021

Published: 19 March 2021

**Publisher's Note:** MDPI stays neutral with regard to jurisdictional claims in published maps and institutional affiliations.



**Copyright:** © 2021 by the authors. Licensee MDPI, Basel, Switzerland. This article is an open access article distributed under the terms and conditions of the Creative Commons Attribution (CC BY) license (<https://creativecommons.org/licenses/by/4.0/>).

## 1. Introduction

Stabilized tetragonal zirconia, as investigated in this study, shows exceptional mechanical properties. Like alumina, it is interesting as part of a wear protection coating of cutting tools in machine material with high cutting speeds. With a high cutting speed, a lot of heat is generated and transferred from the machined material into the tool, decreasing tool life. To minimize this heat transfer, wear protection coatings with oxide ceramics can be used because of their low heat conductivity. Unfortunately, oxides cannot be deposited with standard physical vapor deposition (PVD) processes such as direct current magnetron sputtering or arc evaporation. Most PVD technologies are based on a setting with a material spending cathode (often called a target) and an anode, which is often also the substrate. If the substrate (anode) is coated with a non-conductive material, it vanishes (i.e., the current flow collapses and the electrical discharge disappears). This is also called the disappearing anode effect (DAE). Previous studies by Sellers and Belkind showed possibilities for changed settings to avoid the effect [1,2]. These settings, however, are quite expensive and laborious for application in industry. Instead of changing hardware, this study shows an approach to solving the DAE problem originating from studies of electrical discharge machinable (EDM) ceramics. By alloying oxide ceramics with a percolating electrically conductive dispersion (such as a transition metal carbides), it is possible to obtain an overall electrically conductive ceramic compound [3–7]. In this study, we tried to use this

knowledge in a magnetron sputter process: high-power impulse magnetron sputtering (HiPIMS). HiPIMS, also known as high-power pulsed magnetron sputtering (HPPMS), is the latest iteration of PVD technology, based on direct current magnetron sputtering (DCMS). Like DCMS, an HiPIMS apparatus consists of a sputtering target mounted on a cathode combined with permanent magnets. By ion bombardment, surface atoms from the target material are expelled and accelerated to the anode and the substrate [8]. On the substrate surface, these atoms condense, and a coating is formed. The main difference between DCMS and HiPIMS is the high-frequency pulsing of the cathode, observed by Kouznetsov [9]. By pulsing the cathode with really short pulses (usually 10–100  $\mu$ s), high ion ratios of 90% or more can be reached in HiPIMS. A higher rate of ionized atoms enables different morphologies and therefore better mechanical properties in the coatings [10,11].

The pulse parameters in HiPIMS deposition have a huge impact on the process stability and coating properties. The current at the substrate table, which is a measure for the metal ions that reach the substrate table and build up the coating [8], is measurable with an oscilloscope. However, the current at the substrate table is not only influenced by the pulse parameters of the table, but also by the pulse parameters of the cathode. Depending on the target material and the gas used for the process, different cathode pulse, bias (table) pulse and bias offset values are necessary [12,13].

In this study, the main goal was to examine the impact of five different HiPIMS parameters on the measured current at the substrate table, which is a measure for the metal ions that reach the substrate table and build up the coating.

## 2. Materials and Methods

The parameter study consisted of two parts. First, preliminary tests with the yttria-stabilized zirconia (3YSZ)-titanium carbide (TiC) target on the impact of the working gas flow of argon and krypton on the maximum substrate table current were conducted. In the preliminary tests, the gas flow of argon with respect to krypton varied between 0 and 650 sccm in intervals of 50, which added up to  $14 \times 14 = 196$  individual tests. The frequency was 800 Hz, the on-time of the cathode and the bias was 40  $\mu$ s, and the offset of the bias was 20  $\mu$ s.

Secondly, the main experiments with the 3YSZ-TiC target on the influence of the working gas flow, pulse frequency, cathode on-time, bias on-time and bias offset on the maximum table current were conducted, as shown in Table 1.

**Table 1.** Overview of the high-power impulse magnetron sputtering (HiPIMS) parameters examined in this study. \* Marked parameters were not measured with a gas mix of 150 sccm Ar/0 sccm Kr.

Parameter	Unit	Values
Frequency	Hz	400, 500, 800, 1000 *, 2000 *
On-time cathode	$\mu$ s	20, 30, 40, 50, 60
On-time bias	$\mu$ s	20, 30, 40, 50, 60
Offset bias	$\mu$ s	0, 10, 20, 30, 40, 50, 60, 70, 80

Combined with the four gas mixes picked out for our preliminary tests (150 sccm Ar/0 sccm Kr, 100 sccm Ar/50 sccm Kr, 50 sccm Ar/200 sccm Kr and 0 sccm Ar/550 sccm Kr), we did 4050 tests for our main experiments. The target power was kept constant for the preliminary and main experiments at 4 kW, and the bias voltage was also kept constant at 70 V.

The maximum substrate table current was measured with a Picoscope 4824 oscilloscope produced by Pico Technology Ltd., Saint Neots, United Kingdom, connected to a standard CC800 HiPIMS coating unit produced by CemeCon AG, Würselen, Germany. In order to prevent the DAE and stabilize the coating process, an electrically conductive carbide ceramic (TiC) was added to the 3YSZ target material. The 3YSZ-TiC target contained 30 vol.-% TiC. The 3YSZ-TiC target was hot-pressed and indium bonded by Avaluxe International GmbH, Fürth, Germany.

By measuring the maximum substrate table current, we expected to see which gas flow mix and HiPIMS parameters produced the highest ionization rate of the 3YSZ-TiC target atoms. High ionization is known to lead to better mechanical properties in coatings [14].

To conclude, we prepared coated tungsten carbide specimens with 9 wt-% Co with fixed parameters based on our preliminary experiment, as shown in Table 2.

**Table 2.** Overview of parameters used for the coating of tungsten carbide with cobalt (WC-Co) specimens.

Parameter	Unit	Values
Frequency	Hz	800
On-time cathode	$\mu$ s	40
On-time bias	$\mu$ s	40
Offset bias	$\mu$ s	20
Cathode power	W	4000
Bias voltage	V	70
Gas mix	Sccm	150 Ar/0 Kr
Coating time	s	18,000

Because of non-uniform batch load in production applications (e.g., coating of cutting tools), the average power was kept constant. Peak power and other modes of operation led to deviations in the behavior of the cathode. Big deviations could lead to a security stoppage by the machine system. To measure the maximum table current at a constant set-up, we stopped the table rotation. The batch load was uniform for our measurements.

The coatings were analyzed to measure the coating thickness, hardness, Young's modulus and elemental composition. Elemental composition was also measured on the target material of 3YSZ-TiC.

The thickness measurement (Calo test) was prepared with a Kalottchen/L produced by CemeCon AG, Würselen, Germany and measured with an Olympus BX3M-LEDR light microscope and Olympus Stream software produced by Olympus Europe, Hamburg, Germany.

For the hardness and Young's modulus, we did nanoindentation with a Micro-Combi Tester produced by CSM (now Anton Paar) in Graz, Austria. A total of 24 indentations were executed with a Berkovich indenter. Every indentation was executed with a linear load from 0 to 10 mN at a load rate of 20 mN per minute.

The elemental composition was measured with an XFlash Detector 610M energy dispersive X-ray spectroscope (EDX) produced by Bruker Nano GmbH, Berlin, Germany. The EDX was mounted on an EVO MY 15 scanning electron microscope (SEM) produced by Carl Zeiss Industrielle Messtechnik GmbH, Oberkochen, Germany. The EDX measurements were executed with a 20 kV electron high tension (EHT) and 8.5 cm working distance.

### 3. Results

#### 3.1. Gas Flow

The maximum table current had two high peaks in the low gas flow mix. One peak was observed at 150 sccm argon, 0 sccm krypton (150Ar0Kr) with a maximum table current of 49.1 A, and another was observed at 50 sccm argon and 50 sccm krypton (50Ar50Kr) with a maximum table current of 44.8 A. The 150Ar0Kr showed a stable plasma, while 50Ar50Kr showed arcs on the cathode surface and an unstable (flickering) plasma. It should be noted that while the process was stable at a low gas mix, it was impossible to ignite plasma by directly starting with a low gas mix. Plasma ignition was only possible with a higher gas mix (e.g., 650Ar0Kr). After ignition, the gas mix could be changed to any stable measuring point shown in Figure 1.

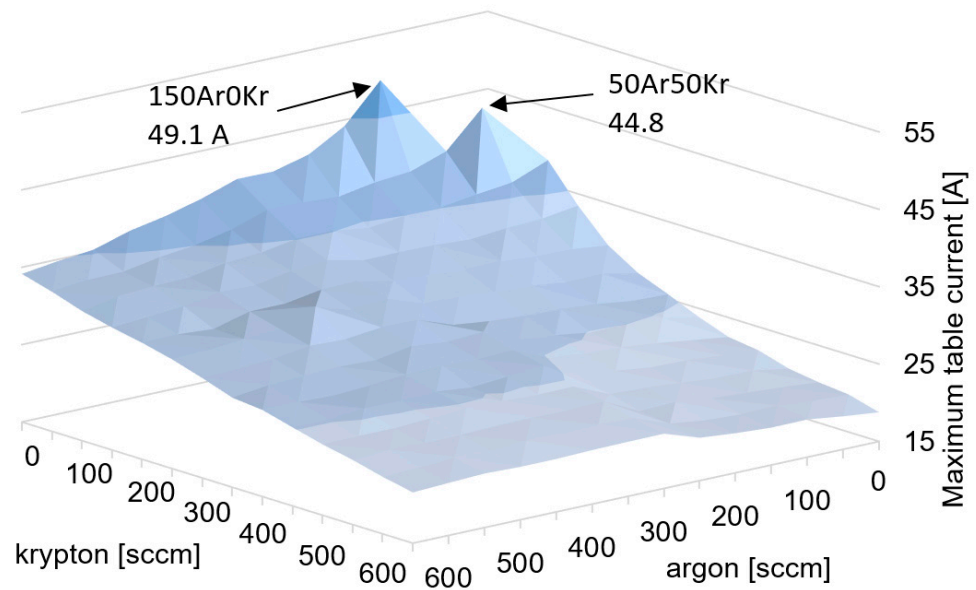


**Figure 1.** Results of the gas flow experiments with yttria-stabilized zirconia (3YSZ)-TiC.

In the parameter field displayed by results of the gas mix measurements (Figure 1), one could not observe any DAE phenomena.

### 3.2. Results of the Parameter Study

In the preliminary experiments with the 3YSZ-TiC target, the measured maximum table current varied between 19 and 49 A. An increasing working gas flow led to a decreasing table current. Krypton had a bigger impact on the current than argon. With a very low working gas flow (argon 0/50/100 sccm, krypton 0 sccm and argon 0 sccm, krypton 50 sccm) the process broke down. Four currents with the respective working gas compositions were chosen for the main experiments, as shown in Table 3.

**Table 3.** Working gas compositions chosen for the main experiments.

Gas Mix	Max. Table Current [A]
150Ar0Kr	49.1
100Ar50Kr	40.1
50Ar200Kr	30.1
0Ar550Kr	20.2

Firstly, we chose the maximum table current of 49 A (argon 150 sccm, krypton 0 sccm) for the main experiments. Secondly, we selected a very low table current of 20 A (argon 0 sccm, krypton 550 sccm). Finally, we picked two currents in the lower and higher mid-table at 30 and 40 A (argon 100 sccm, krypton 50 sccm and argon 50 sccm, krypton 200 sccm).

We could not observe a stable plasma at 400 Hz with any mix of pulse parameters. In general, we could observe decreasing maximum table currents with increasing gas loads. With an increasing frequency, we could observe decreasing values of the maximum table currents, with 500 Hz showing the highest maximum table currents. The highest value measured was 152 A at 150Ar0Kr, 500 Hz, a 20  $\mu$ s on-time cathode, a 50  $\mu$ s on-time bias and a bias offset of 20  $\mu$ s. The minimum measured was 3 A at 0Ar550Kr, 2000 Hz, an on-time cathode of 60  $\mu$ s, an on-time bias of 30  $\mu$ s and a 0  $\mu$ s offset.

Figure 2 shows all results of the 500 Hz measurements with different on-time cathodes at 150Ar0Kr. One can see that the maximum table currents increased with the decreasing on-time values of the cathode.

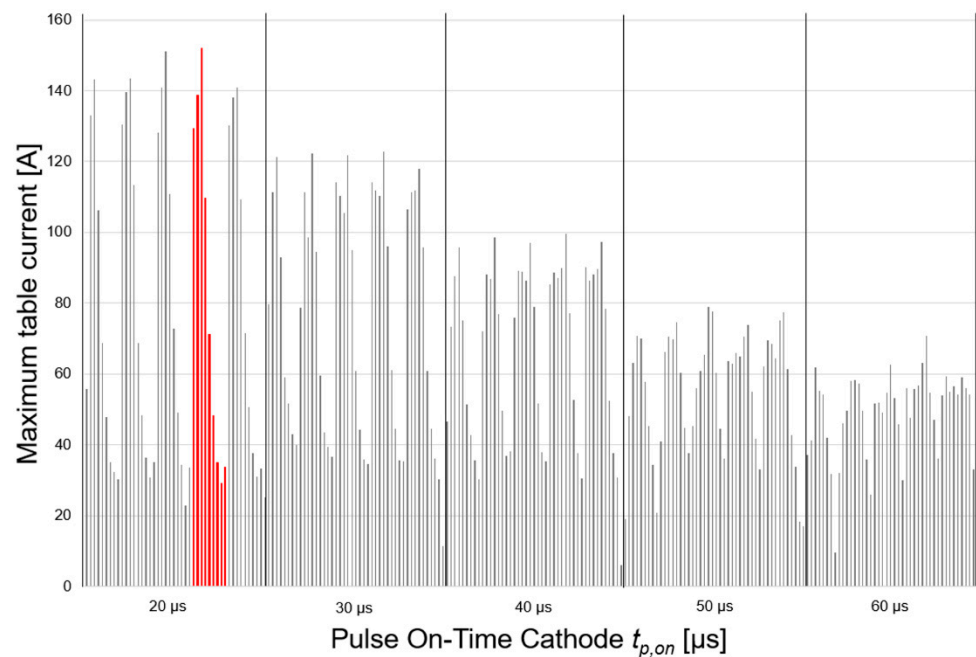


**Figure 2.** Results of all 500 Hz measurements with different pulse on-time values of the cathode with a 150Ar0Kr gas mix. The red highlighted measurements are the results of the bias offset range 0–80  $\mu\text{s}$  with 150Ar0Kr at 500 Hz, a 20  $\mu\text{s}$  cathode on-time and a bias on-time of 50  $\mu\text{s}$ , which is also shown in Figure 3.

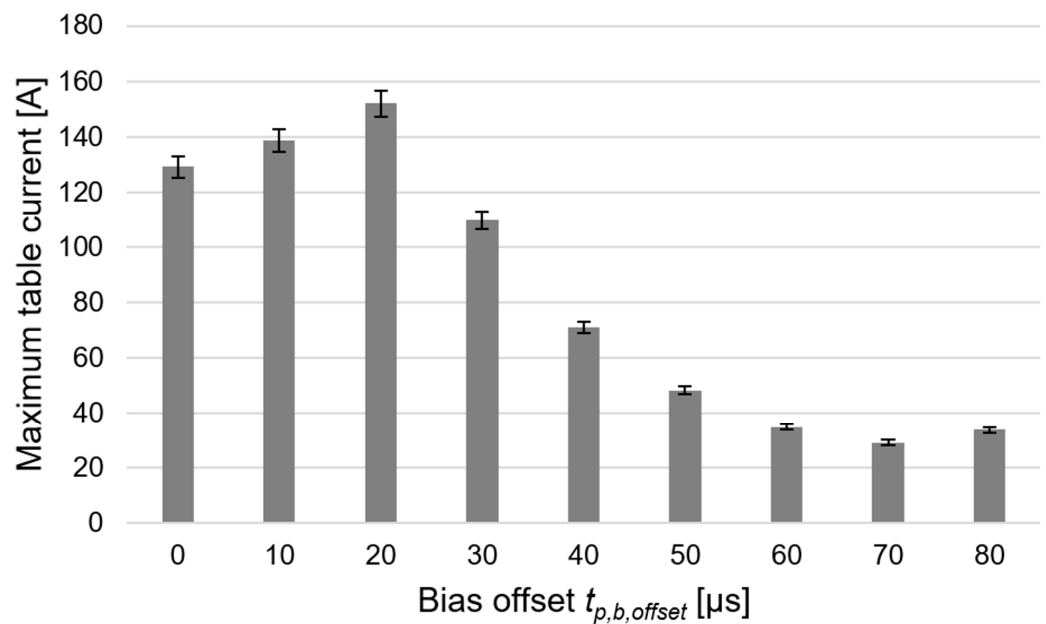


**Figure 3.** Results of bias offset at 150Ar0Kr, 500 Hz, a cathode on-time of 20  $\mu\text{s}$  and a bias on-time of 50  $\mu\text{s}$ .

An increasing on-time of the cathode with other parameters kept constant led to a decrease of the table current. The maximum table current for the 20  $\mu\text{s}$  cathode on-time was approximately twice the maximum table current for the 60  $\mu\text{s}$  on-time. The on-time of the bias had no measurable impact on the maximum current at the substrate table. For measurements of the bias offset, the results did not show linear behavior. Figure 3 shows the results of the bias offset with 150Ar0Kr at 500 Hz, a cathode on-time of 20  $\mu\text{s}$  and a bias on-time of 50  $\mu\text{s}$ .

One can observe an increase of the maximum table current from 130 A to 152 A with an increase in the bias offset. With a further increase of the bias offset beyond 20  $\mu\text{s}$ , the maximum table current decreased rapidly.

The offset had a bigger impact on the maximum table current for the lower bias on-times than for the higher ones. Moreover, the bias on-time had an influence on the ideal offset, meaning the offset with the highest maximum table current. The ideal offset varied between 30 and 60  $\mu\text{s}$ , with 30  $\mu\text{s}$  being mostly for a low bias on-time and 60  $\mu\text{s}$  for a high bias on-time. A low on-time of the bias caused more arcs and less process stability. In addition, at low offsets between 0 and 30  $\mu\text{s}$ , as well as high offsets between 60 and 80  $\mu\text{s}$ , most arcs were detected.

The highest maximum table currents are shown in Table 4.

**Table 4.** Highest values of the maximum table currents. All measurements were executed with a 500 Hz HiPIMS frequency.

Gas Mix	$t_{p,on}$ ( $\mu\text{s}$ )	$t_{s,on}$ ( $\mu\text{s}$ )	$t_s$ , Offset ( $\mu\text{s}$ )	Max. Table Current (A)
150Ar0Kr	20	50	20	152.1
100Ar50Kr	30	40	30	114.1
50Ar200Kr	30	60	30	79.6
0Ar550Kr	20	40	20	56.7

### 3.3. Results of the Coating Analyzation

Table 5 shows the mechanical property results of our coating measured with nanoindentation and calo tests.

**Table 5.** Mechanical properties of a 3YSZ-titanium carbide (TiC) coating on WC-Co specimens.

Property	Unit	Values
Hardness	GPa	$24.5 \pm 2.5$
Young's modulus	GPa	$415 \pm 44$
Thickness	$\mu\text{m}$	$0.9 \pm 0.1$

The compositions of the target material and coating are compared in Table 6.

**Table 6.** Atomic composition (as a percentage) of the 3YSZ-TiC target material and coating.

Element	Target	Coating
Carbon (C)	$24.7 \pm 2.1$	$29.2 \pm 1.1$
Oxygen (O)	$47.0 \pm 4.1$	$34.5 \pm 1.5$
Titanium (Ti)	$11.7 \pm 0.6$	$15.1 \pm 0.5$
Yttrium (Y)	$0.7 \pm 0.1$	$1.3 \pm 0.3$
Zirconium (Zr)	$15.9 \pm 2.0$	$19.9 \pm 1.5$

## 4. Discussion

A parameter study based on the HiPIMS parameters of the working gas flow, frequency, on-time cathode, on-time bias and offset bias was conducted, and the influence of the mentioned parameters on the measured current at the substrate table was determined.

As expected, by using the conductive target material, the disappearing anode effects were not observed during all of our measurements.

The authors did not expect a maximum table current with a low gas load, as shown in Figure 1. However, one can interpret the low gas load as the formation of a third working gas, presumably consisting of carbon monoxide, which is produced by the decomposition of the target itself. With this autogenously formed working gas, the maximum table currents at an expected unstable gas mix of argon and krypton are possible. Zirconia

(ZrO<sub>2</sub>) and titanium carbide (TiC) are known for their reactive behavior with each other in high-energy environments [15], so it is possible that the oxygen from ZrO<sub>2</sub> reduces the TiC and takes part in the sputtering process as a third working gas.

In our study, we also tried to restart the plasma with a low gas load, and it did not ignite, another indication of the formation of a carbon monoxide gas from the target material. The EDX measurements strengthen this theory, because the coating lost a significant amount of oxygen. The EDX values of carbon are often not that reliable. Another theory behind the high currents is based on HiPIMS technology. The two peaks in the gas flow mix measurements are probably a case of a dominating self-sputtering mechanism, based on the Anders model of self-sputtering shown elsewhere [16]. With a high gas load mix, the gas sputtering of argon and krypton dominates the process. Due to the low ionization energy of metals (here zirconium and titanium) compared with argon, the concentration of the doubly charged metal ions of the sputtered species is expected to be high [17]. High doubly charged metal ions are necessary for the self-sputtering process. Like Andersson and Anders, we needed an ignition phase of the plasma [18,19]. In our case, we started our discharge with a higher gas mix. By reducing our gas mix (e.g., 150 sccm Ar, 0 sccm Kr), we sponsored the shift from gas sputtering to self-sputtering. The dominating metal ion species created more and more secondary electrons and led to high discharge currents. The currents measured at the table were also an indication of the self-sputtering runaway described by Anders and Gudmundsson [16,17]. The high flux of metal ions increased the sputtering due to the self-sputtering, and more neutral target atoms can be ionized, which also can participate in the self-sputtering and contribute to the high current measurements.

The main experiments of the parameter study support the results from the preliminary experiments with regard to the influence of the working gas flow. Furthermore, the table current decreased with the increasing frequency because of the decreasing cathode peak power. Increasing the frequency reduced the off-time of the cathode and the charging time of the capacitor bank for the next cathode pulse. The lower peak power was also the cause of the decreasing current with the increasing pulse width. The authors plan to investigate the speculated formation of a third working gas in a future study to classify the ratio of self-sputtering and working gas formation of the results.

With a frequency of 400 Hz, the process could not be stabilized. The higher the on-time of the cathode, the lower the measured maximum table current was. With lower on-times, more arcs occurred, and the process was less stable. The on-time of the bias had no significant impact on the table current.

Nevertheless, the ideal offset of the bias pulse depended on the bias on-time. This offset value lay in the range of 30 and 50  $\mu$ s, with 30  $\mu$ s being mostly for a low bias on-time and 50  $\mu$ s for a high bias on-time. The low bias on-times decreased the time, and ions were actively forced to move to the substrate table by the bias pulse. High bias on-times decreased the maximum table current and increased contamination of the coating with non-ionized atoms. However, as shown in Table 4, the highest maximum table currents could be reached with a 40–60  $\mu$ s bias on-time and a 20–30  $\mu$ s bias offset.

Most arcs, as well as the highest process instability, were found especially for the low bias on-times between 20 and 30  $\mu$ s, in addition to the low (0–30  $\mu$ s) or high (60–80  $\mu$ s) bias offsets.

Further experiments should show the influence of the maximum table current on the mechanical properties of the coating, and the assumption of the formation of carbon-oxide gas out of the target material needs to be confirmed.

The measured mechanical properties of the coating observed were higher than in other studies. Keshavarz et al. deposited pure yttrium-stabilized zirconia with electron beam physical vapor deposition (EB-PVD) and found a measured hardness up to almost 22 GPa [20]. Thermal spray coatings of YSZ are often spongy, owing to their use as a thermal barrier coating, with a low hardness up to 800 HV and a Young's modulus no greater than 95 GPa [21,22]. Due to the good process capability and promising mechanical properties, further experiments could reduce the TiC addition in the target material, because the

electrical conductivity of oxide-based EDM ceramics rises with a volume fraction of 20 TiC from a few thousand S/m to over 20 kS/m with 28 vol.-% TiC, as reported for ZTA [6].

## 5. Conclusions

By mixing a non-conductive oxide ceramic like 3YSZ with a conductive ceramic like TiC as a target material, one can avoid any disappearing anode effects (DAEs) without changing any other hardware of a coating unit. The lack of the DAE and the successful deposition of 3YSZ-TiC-based coatings confirm the process capability of our approach.

Our main focus was an HiPIMS parameter study to observe the maximum table current with different pulse parameters and gas mixes. One could observe the highest ionized target material reaching the substrate table at low gas mixes, which we led back to a runaway self-sputtering mechanism. We also propose the production of a third process gas out of oxygen and carbon, which reacted out of the target material. In our HiPIMS parameter study, the highest maximum substrate table currents (up to 152 A) were also observed with the lowest possible gas mix (150 sccm argon, 0 sccm krypton).

**Author Contributions:** Conceptualization, B.G.; data curation, S.G.; investigation, S.G.; methodology, B.G.; project administration, R.G.; supervision, B.G.; validation, F.K., A.K. and R.G.; visualization, B.G.; writing—original draft, B.G.; writing—review and editing, F.K. All authors have read and agreed to the published version of the manuscript.

**Funding:** This research received no external funding.

**Institutional Review Board Statement:** Not applicable.

**Informed Consent Statement:** Not applicable.

**Data Availability Statement:** The data presented in this study are openly available in Figshare at <https://doi.org/10.6084/m9.figshare.14237402>.

**Acknowledgments:** The authors gratefully acknowledge the financial support of the project by Lothar and Markus Horn, Hartmetall-Werkzeugfabrik Paul Horn GmbH, Tübingen, Germany.

**Conflicts of Interest:** The authors declare no conflict of interest. The funders had no role in the design of the study; in the collection, analyses, or interpretation of data; in the writing of the manuscript, or in the decision to publish the results.

## References

1. Sellers, J.C. The disappearing anode myth: Strategies and solutions for reactive PVD from single magnetrons. *Surf. Coat. Technol.* **1997**, *94–95*, 184–188. [[CrossRef](#)]
2. Belkind, A.; Zhao, Z.; Scholl, R. Dual-anode magnetron sputtering. *Surf. Coat. Technol.* **2003**, *163–164*, 695–702. [[CrossRef](#)]
3. Landfried, R.; Kern, F.; Gadow, R. Development of Electrical Discharge Machinable ZTA Ceramics with 24 vol% of TiC, TiN, TiCN, TiB<sub>2</sub> and WC as Electrically Conductive Phase. *Int. J. Appl. Ceram. Technol.* **2013**, *10*, 509–518. [[CrossRef](#)]
4. Landfried, R.; Kern, F.; Gadow, R. Electrically conductive ZTA-TiC ceramics: Influence of TiC particle size on material properties and electrical discharge machining. *Int. J. Refract. Met. Hard Mater.* **2015**, *49*, 334–338. [[CrossRef](#)]
5. Schmitt-Radloff, U.; Kern, F.; Gadow, R. Wire-electrical discharge machinable alumina zirconia niobium carbide composites—Influence of NbC content. *J. Eur. Ceram. Soc.* **2017**, *37*, 4861–4867. [[CrossRef](#)]
6. Schmitt-Radloff, U.; Gommeringer, A.; Assmuth, P.; Kern, F.; Klocke, F.; Holsten, M.; Schneider, S. Effects of composition on mechanical and ED-machining characteristics of zirconia toughened alumina-titanium carbide (ZTA-TiC) composite ceramics. *Procedia Cirp.* **2018**, *68*, 17–21. [[CrossRef](#)]
7. Gommeringer, A.; Schmitt-Radloff, U.; Ninz, P.; Kern, F.; Klocke, F.; Schneider, S.; Holsten, M.; Klink, A. ED-machinable ceramics with oxide matrix: Influence of particle size and volume fraction of the electrical conductive phase on the mechanical and electrical properties and the EDM characteristics. *Procedia Cirp.* **2018**, *68*, 22–27. [[CrossRef](#)]
8. Anders, A. Tutorial: Reactive high power impulse magnetron sputtering (R-HiPIMS). *J. Appl. Phys.* **2017**, *121*, 171101. [[CrossRef](#)]
9. Kouznetsov, V.; Macák, K.; Schneider, J.M.; Helmersson, U.; Petrov, I. A novel pulsed magnetron sputter technique utilizing very high target power densities. *Surf. Coat. Technol.* **1999**, *122*, 290–293. [[CrossRef](#)]
10. Anders, A. A structure zone diagram including plasma-based deposition and ion etching. *Thin Solid Film.* **2010**, *518*, 4087–4090. [[CrossRef](#)]

11. Čada, M.; Britun, N.; Hecimovic, A.; Gudmundsson, J.T.; Lundin, D. Heavy species dynamics in high power impulse magnetron sputtering discharges. In *High Power Impulse Magnetron Sputtering*, 1st ed.; Lundin, D., Minea, T., Gudmundsson, J.T., Eds.; Elsevier: Amsterdam, The Netherlands, 2020; pp. 111–126.
12. Greczynski, G.; Lu, J.; Jensen, J.; Petrov, I.; Greene, J.E.; Bolz, S.; Koelker, W.; Schiffers, C.; Lemmer, O.; Hultman, L. Metal versus rare-gas ion irradiation during Ti1-xAlxN film growth by hybrid high power pulse magnetron/dc magnetron co-sputtering using synchronized pulsed substrate bias. *J. Vac. Sci. Technol. A* **2012**, *30*, 061504. [[CrossRef](#)]
13. Brenning, N.; Butler, A.; Hajihoseini, H.; Rudolph, M.; Raadu, M.A.; Gudmundsson, J.T.; Minea, T.; Lundin, D. Optimization of HiPIMS discharges: The selection of pulse power, pulse length, gas pressure, and magnetic field strength. *J. Vac. Sci. Technol. A* **2020**, *38*, 033008. [[CrossRef](#)]
14. Greczynski, G.; Lu, J.; Jensen, J.; Petrov, I.; Greene, J.E.; Bolz, S.; Kölker, W.; Schiffers, C.; Lemmer, O.; Hultman, L. Strain-free, single-phase metastable Ti0.38Al0.62N alloys with high hardness: Metal-ion energy vs. momentum effects during film growth by hybrid high-power pulsed/dc magnetron cosputtering. *Thin Solid Film*. **2014**, *556*, 87–98. [[CrossRef](#)]
15. Vleugels, J.; Van der Biest, O. Development and Characterization of Y<sub>2</sub>O<sub>3</sub>-Stabilized ZrO<sub>2</sub> (Y-TZP) Composites with TiB<sub>2</sub>, TiN, TiC, and TiC<sub>0.5</sub>N<sub>0.5</sub>. *J. Am. Ceram. Soc.* **1999**, *82*, 2717–2720. [[CrossRef](#)]
16. Anders, A.; Čapek, J.; Hála, M.; Martinu, L. The ‘recycling trap’: A generalized explanation of discharge runaway in high-power impulse magnetron sputtering. *J. Phys. D Appl. Phys.* **2012**, *45*, 012003. [[CrossRef](#)]
17. Gudmundsson, J.T.; Brenning, N.; Lundin, D.; Helmersson, U. High power impulse magnetron sputtering discharge. *J. Vac. Sci. Technol. A Vac. Surf. Films* **2012**, *30*, 030801. [[CrossRef](#)]
18. Andersson, J.; Anders, A. Gasless sputtering: Opportunities for ultraclean metallization, coatings in space and propulsion. *Appl. Phys. Lett.* **2008**, *92*, 221503. [[CrossRef](#)]
19. Andersson, J.; Anders, A. Self-Sputtering Far above the Runaway Threshold: An Extraordinary Metal-Ion Generator. *Phys. Rev. Lett.* **2009**, *102*, 045003. [[CrossRef](#)] [[PubMed](#)]
20. Keshavarz, M.; Idris, M.H.; Ahmad, N. Mechanical properties of stabilized zirconia nanocrystalline EB-PVD coating evaluated by micro and nano indentation. *J. Adv. Ceram.* **2013**, *2*, 333–340. [[CrossRef](#)]
21. Lima, R.S.; Kucuk, A.; Berndt, C.C. Evaluation of microhardness and elastic modulus of thermally sprayed nanostructured zirconia coatings. *Surf. Coat. Technol.* **2001**, *135*, 166–172. [[CrossRef](#)]
22. Portinha, A.; Teixeira, V.; Carneiro, J.; Martins, J.; Costa, M.F.; Vassen, R.; Stoever, D. Characterization of thermal barrier coatings with gradient in porosity. *Surf. Coat. Technol.* **2005**, *195*, 245–251. [[CrossRef](#)]